Tensor Analyzing Power in *pd* Backward Scattering at GeV Energies

G. Igo and M. Bleszynski
Department of Physics, University of California at Los Angles, Los Angeles, California 90024

and

J. B. Carroll
Department of Physics, University of California at Los Angeles, Los Angeles, California 90024, and Lawrence Berkeley Laboratory, Berkeley, California 94720

and

A. Sagle
Lawrence Berkeley Laboratory, Berkeley, California 94720

and

C. L. Morris
Los Alamos Scientific Laboratory, Los Alamos, New Mexico 87545

and

R. Klem
Argonne National Laboratory, Argonne, Illinois 60439

and

T. Joyce, Y. Makdisi, M. Marshak, B. Mossberg, E. A. Peterson, K. Ruddick, and J. Whittaker
Department of Physics, University of Minnesota, Minneapolis, Minnesota 55455
(Received 19 March 1979)

Measurements are reported of the spherical tensor component t_{20} for 1.0-, 0.8-, and 0.4-GeV equivalent proton bombarding energies for elastic p-d scattering between 155°–175°. They are very close to zero in disagreement with the predictions of nucleon exchange models, including the Kerman-Kisslinger model with N^* components in the deuteron wave function. The experiment was performed with a vector- and tensor-polarized deuteron beam scattered from a liquid hydrogen target.

The existence of a peak in the backward cross section for p-d and n-d scattering in the GeV energy range has produced considerable theoretical speculation. Kerman and Kisslinger[1] have proposed that near 1 GeV, N^* components in the deuteron wave function augment the amplitudes as a result of neutron exchange (KK model). The shoulder (near 600 MeV), seen very clearly in a recent n-d scattering experiment,[2] has been explained by a higher-order Feynman (triangle) diagram[3-5] involving the exchange of an $N^*(1232)$ in the π-p s channel. The complexity of the scattering mechanism is indicated by two recent experiments[6,7] which measured the analyzing power for the backward (but not 180°) scattering of polarized protons from a deuterium target. The maximum asymmetry was measured at the shoulder in the backward cross section; a smaller analyzing power was observed for both higher and lower energies. A similarity was found in the magnitude of the analyzing powers for backward p-d scattering and for the reaction $p+p\rightarrow d+\pi$, but the two were by no means algebraically equal. The authors[6,7] concluded that all mechanisms described above may enter into the backward-scattering process in the GeV energy region.

Although the vector analyzing power and most components of the tensor analyzing power must vanish at 180° by general symmetry arguments,[8] the component t_{20} of the spherical tensor analyzing power may remain finite.[9] Vasan[8] has shown if the elastic scattering near 180° goes by the KK mechanism, that t_{20} will be generally large in magnitude and have a strong energy dependence between 0.4- and 1.0-GeV proton bombarding energy. Also we find t_{20} calculated from direct scattering mechanism is appreciable at 180° because of the large-angle behavior of the n-n amplitudes.

Deuteron beams of $p_d = 3.4$, 2.9, 2.4, and 1.9 GeV/c were produced at the Argonne Zero-Gradient Synchrotron (ZGS) with tensor and vector components oriented along the y axis in our coordinate system, normal to the scattering plane. By utilizing a pair of superconducting solenoids in the beam line, these components could be precessed into the scattering plane along the x axis, normal to the beam direction (z axis). In either case, a pattern of four pulses [rate $\sim(3\text{ s})^{-1}$, width ~ 1 s] each with a different combination of signs for the vector polarization, using the Madison convention,[9] of magnitude p_y (p_x), and tensor alignment of magnitude p_{yy} (p_{xx}), was repeatedly produced with the superconducting solenoids in the beam line off (on). Our detection system was a high-resolution spectrometer[10] oriented to the left, looking downstream in the x-z plane. The differential cross section with the solenoids off is

$$(d\sigma/dt)_{\uparrow(\downarrow),\uparrow(\downarrow)} = (d\sigma/dt)_{\text{unpol}}[1 \pm p_y \tfrac{3}{2}\mathcal{P}_y \pm p_{yy}\tfrac{1}{2}\mathcal{P}_{yy}], \tag{1}$$

where the up and down arrows (first subscript) which indicate the direction of the vector polarization are associated with the plus and minus signs, respectively, on the second term on the right-hand side; the up and down arrows (second subscript) which indicate the tensor alignment are associated with the plus and minus signs, respectively, on the third term. The differential cross section with the solenoid on is

$$(d\sigma/dt)_{\uparrow(\downarrow),\uparrow(\downarrow)} = (d\sigma/dt)_{\text{unpol}}[1 \pm p_x \tfrac{3}{2}\mathcal{P}_x \pm p_{xx}\tfrac{1}{2}\mathcal{P}_{xx}], \tag{2}$$

with a notation similar to that in Eq. (1). In Eqs. (1) and (2), $\mathcal{P}_y$, $\mathcal{P}_x$ and $\mathcal{P}_{yy}$, $\mathcal{P}_{xx}$ are the Cartesian components of the induced vector and tensor analyzing powers, respectively.[9] Since p_x is in the scattering plane, $\mathcal{P}_x$ should vanish because of time-reversal- and parity-invariance symmetries. The full measurements obtained for $\mathcal{P}_x$ given in Table I serve as a check on our measurements. The tensor quantities extracted from A ($\equiv Y_{\uparrow,\uparrow}/I_{\uparrow,\uparrow}$), B ($\equiv Y_{\downarrow,\uparrow}/I_{\uparrow,\downarrow}$), C ($\equiv Y_{\uparrow,\downarrow}/I_{\downarrow,\uparrow}$), and D ($\equiv Y_{\uparrow,\downarrow}/I_{\downarrow,\uparrow}$) of the measured yields $Y_{\uparrow(\downarrow),\uparrow(\downarrow)}$ and beam fluxes $I_{\uparrow(\downarrow),\uparrow(\downarrow)}$ are

$$p_y\tfrac{3}{2}\mathcal{P}_y = [(A+B)-(C+D)]/[(A+B)+(C+D)] \quad \text{(solenoids off)}, \tag{3a}$$

$$p_{yy}\tfrac{1}{2}\mathcal{P}_{yy} = [(A+C)-(B+D)]/[(A+C)+(B+D)] \quad \text{(solenoids off)}, \tag{3b}$$

$$p_{xx}\tfrac{1}{2}\mathcal{P}_{xx} = [(A+C)-(B+D)]/[(A+B)+(C+D)] \quad \text{(solenoids on)}, \tag{3c}$$

$$p_x\tfrac{3}{2}\mathcal{P}_x = [(A+B)-(C+D)]/[(A+B)+(C+D)] \quad \text{(solenoids on)}. \tag{3d}$$

The beam intensity was 10^8–3×10^9 per pulse. The target was a 10-cm flask containing liquid hydrogen. The direction, positions, and emittance of the incident beam were determined by four multiwire proportional counters read out in an integrated mode. The relative beam intensity was monitored independently of spin effects by three ion chambers, which tracked to within 3%. The absolute value of the tensor alignment was measured at the source using the large left-right asymmetry in the neutrons produced by the d-t reaction near 100 keV.[11] This parameter was measured frequently over the course of the measurements, a total of eleven times. The magnitude was 0.75 ± 0.03 for the majority of the measurements and was equal for positive and negative values within the uncertainty (± 0.03). From the source dynamics, the absolute value of the vector polarization is also established at the value of 0.25 with the same fractional uncertainty. Relative values of the beam's vector polarization were determined with an uncertainty of $\pm 4\%$ by a CH_2 target polarimeter located at the point at which the deuterons were extracted from the ZGS. Relative values of the alignment and polarization and in addition the accuracy of the spin precession were monitored using a CH_2 target polarimeter placed between the solenoids and the target. Left, right, up, and down forward-recoil telescopes identified d-p elastic events. These rates were particularly sensitive to p_{yy} (p_{xx}). Recoil alone rates, presumably dominated by inelastic scattering, were more dependent on p_y (p_x). The relative uncertainties of these quantities were 0.05. No depolarizing resonances were passed through in the process of acceleration to the momenta used in this experiment.[12] Depolarization effects are generally expected to be negligible since the magnetic moment is one-third as large as that of the proton. No depolarization of proton beams was found in earlier experiments.[7,10] Particle identification was effected by using the momentum resolution of the spectrometer and time-of-flight selection utilizing a 15-m flight path. The spatial distribution of the events selected

TABLE I. Summary of asymmetry measurements at backward angles in the c.m. system (θ^* near 180°). Measured values with target full contain contributions from both liquid hydrogen and the flask walls. The standard errors reflect statistical uncertainties only.

3.4 GeV/c (1 GeV Equivalent Proton Bombarding Energy)

θ^* (degrees)	$p_{yy}\frac{1}{2}\mathcal{P}_{yy}$	$p_y\frac{3}{2}\mathcal{P}_y$	$p_{xx}\frac{1}{2}\mathcal{P}_{xx}$	$p_x\frac{3}{2}\mathcal{P}_x$	Target
155	+0.021±0.017	+0.013±0.018			Full
160	−0.011±0.017	+0.023±0.016			Full
165	−0.008±0.013	+0.037±0.012			Full
165	+0.078±0.050	+0.019±0.050	−0.004±0.099	+0.007±0.009	Empty
175	−0.002±0.012	+0.029±0.012	+0.018±0.012 −0.004±0.009	−0.017±0.013 +0.007±0.009	Full
175	−0.028±0.029	−0.007±0.030			Empty

2.9 GeV/c (800 MeV Equivalent Proton Bombarding Energy)

θ^* (degrees)	$p_{yy}\frac{1}{2}\mathcal{P}_{yy}$	$p_y\frac{3}{2}\mathcal{P}_y$	$p_{xx}\frac{1}{2}\mathcal{P}_{xx}$	$p_x\frac{3}{2}\mathcal{P}_x$	Target
170	−0.020±0.021 +0.046±0.044	−0.039±0.021 −0.003±0.044	0.029±0.015	−0.012±0.015	Full
170	+0.013±0.030	0.008±0.030			Empty
175	+0.012±0.020 −0.017±0.016 +0.013±0.015 +0.017±0.018	−0.008±0.020 −0.034±0.016 +0.009±0.015 −0.008±0.018	−0.014±0.015 +0.043±0.031 +0.022±0.033 +0.043±0.038	+0.003±0.015 +0.013±0.031 +0.011±0.033 +0.049±0.038	Full
175	+0.002±0.020	−0.015±0.020	+0.012±0.022	0.041±0.022	Empty

2.4 GeV/c (600 MeV Equivalent Proton Bombarding Energy)

θ^* (degrees)	$p_{yy}\frac{1}{2}\mathcal{P}_{yy}$	$p_y\frac{3}{2}\mathcal{P}_y$	$p_{xx}\frac{1}{2}\mathcal{P}_{xx}$	$p_x\frac{3}{2}\mathcal{P}_x$	TGT Flask
175	+0.032±0.044 −0.001±0.016	−0.039±0.044 0.011±0.016	−0.031±0.014	+0.011±0.014	Full
175	+0.002±0.011	+0.010±0.011	−0.019±0.010	−0.015±0.010	Empty

1.9 GeV/c (400 MeV Proton Equivalent Bombarding Energy)

θ^* (degrees)	$p_{yy}\frac{1}{2}\mathcal{P}_{yy}$	$p_y\frac{3}{2}\mathcal{P}_y$	$p_{xx}\frac{1}{2}\mathcal{P}_{xx}$	$p_x\frac{3}{2}\mathcal{P}_x$	TGT Flask
175	0.032±0.043 0.018±0.079	−0.007±0.043 −0.032±0.079	−0.015±0.032	−0.037±0.032	Full
175	−0.082±0.069	−0.068±0.069			Empty

was examined using drift chambers placed at the final focal plane. Data points taken with the target full and empty at center-of-mass angles θ^* are listed in Table I. The typical magnitude of the target-empty scattering rate varied between 20% of the target-full rate at 3.4 GeV/c to 90% at 1.9 GeV/c. At 1.9 GeV/c, the elastic deuteron's kinetic energy is relatively low and multiple-scattering losses in the target, scintillators, and other materials become significant. An inspection of the data for all incident momenta between 3.4 GeV/c (equivalent proton bombarding energy, 1 GeV) and 1.9 GeV/c (equivalent proton bombarding energy, 0.4 GeV) shows that *all target-full and target-empty measurements are consistent with zero tensor and vector induced polarizations,* and independent of scattering angle between 155° and 175° (c.m.), in contrast to theoretical expectations. A number of systematic checks were made on the validity of the data. Data-collection runs at identical scattering angles spaced by several days in real time yielded consistent results. Interspersed among the runs were measurements of forward p-d scattering which yield large vector and tensor analyzing powers indicating the beam was polarized. Values of $\mathcal{P}_x$ at backward angles (Table I) and also at forward angles where the true asymmetries were large, were consistent with the expected value of zero. The measured vector analyzing power at backward angles was zero as required by symmetry. The rapid reversal of the polarities of the vector and tensor components of the beam ensured cancellation of effects due to apparatus drifts with a period long compared to 12 s. No evidence was found for structure in the position or size of the beam which was correlated within the incident beam's polarization or alignment.

TABLE II. The tensor and vector components $\mathcal{P}_{yy}$, $\mathcal{P}_{xx}$, t_{20} [Eqs. (4a) and (4b), and $\mathcal{P}_x$ and $\mathcal{P}_y$ for hydrogen extracted from measurements at backward angles in the c.m. system (θ^* near 180°). The standard errors reflect statistical errors only.

p_d (GeV/c)	θ^* (deg)	$\mathcal{P}_{yy}$	t_{20}	$\mathcal{P}_y$	$\mathcal{P}_{xx}$	t_{20}	$\mathcal{P}_x$
3.45	165	-0.057 ± 0.033	$+0.080\pm0.050$	-0.037 ± 0.035			
3.45	175	-0.009 ± 0.030	$+0.012\pm0.042$	0.029 ± 0.029			
2.95	170				-0.015 ± 0.033	$+0.022\pm0.050$	-0.048 ± 0.052
2.95	175	0.000 ± 0.030	0.000 ± 0.042	0.06 ± 0.023	-0.042 ± 0.030	$+0.060\pm0.046$	-0.040 ± 0.048
1.9	175	0.147 ± 0.111	-0.200 ± 0.160	0.008 ± 0.011			

Because the product terms in Table I are so small, we can extract the absolute values of $\mathcal{P}_y$, $\mathcal{P}_{yy}$, $\mathcal{P}_x$, and $\mathcal{P}_{xx}$ for hydrogen (Table II) obtained by subtraction of normalized target-empty runs from target-full runs, using the nominal values of p_x (p_y) and p_{yy} (p_{xx}). The absolute and relative uncertainties of these are small compared with the statistical errors. Recalling that t_{22} is identically zero at 180°, our measurements of $\mathcal{P}_{yy}$ and $\mathcal{P}_{xx}$ become direct measurements of t_{20} since[8]

$$\mathcal{P}_{xx} = \sqrt{3}\, t_{22} - \frac{1}{\sqrt{2}} t_{20}, \tag{4a}$$

$$\mathcal{P}_{yy} = -\sqrt{3}\, t_{22} - \frac{1}{\sqrt{2}} t_{20}. \tag{4b}$$

At 2.9 GeV/c, both $\mathcal{P}_{xx}$ and $\mathcal{P}_{yy}$ for d-p scattering were extracted from the data. Using Eqs. (4a) and (4b), we obtain $t_{22} = -0.026\pm0.021$ and $t_{20} = -0.020\pm0.022$, confirming the expected result that t_{22} is zero.

Experimental results for equivalent proton bombarding energies of 0.4, 0.8, and 1 GeV are shown in Fig. 1. We could not extract a value for t_{20} at 0.6 GeV since corresponding target-full and target-empty runs, taken under equivalent trigger conditions, were not available. However, as stated above, measurements at 0.6 GeV both for target-full and for target-empty runs were consistent with zero tensor polarization. The data at 0.4, 0.8, and 1 GeV for t_{20} are compared in Fig. 1 with the prediction of Vasan[8] with and without the N^* component of the deuteron. It is clear that the agreement is poor. Because of the finite width of the $N^*(1232)$ resonance, the triangle graph model would also show some energy dependence. Indeed, it is likely that any naive nucleon-exchange model, which can account for the shoulder in the energy dependence of the backward cross section, should show some energy dependence in t_{20}. The vanishing of this component of the tensor analyzing power should therefore place strong constraints upon proposed models for backward p-d scattering.

We are deeply indebted to the staff of the Argonne ZGS. This work was supported in part by the U. S. Department of Energy. One of us (M.B.) expresses his gratitude for support to the T-5 and MP Divisions of the Los Alamos Scientific Laboratory, where part of this work was done.

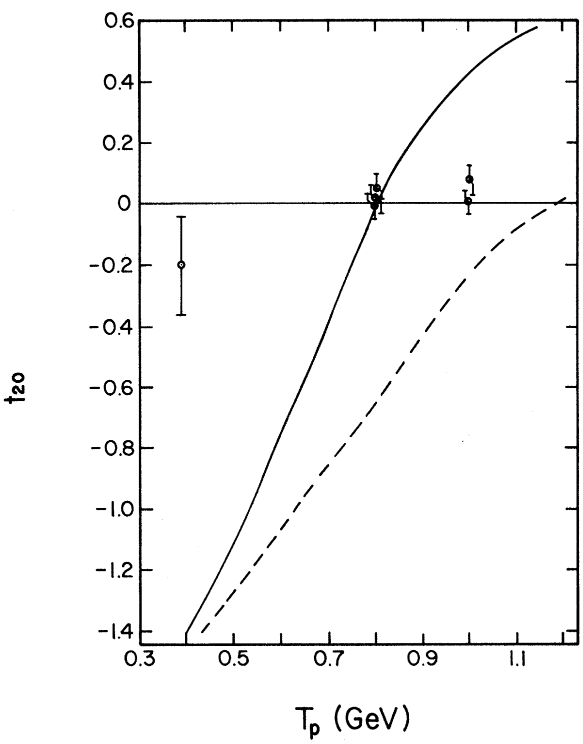

FIG. 1. Dependence of the spherical tensor component t_{20} on equivalent proton bombarding energy. The curves are taken from Ref. 8. The dashed curve is evaluated with $S+D$ (6.5%) components in the deuteron model wave function. The solid curve uses a model wave function with an additional D^* (1.6%) component described in the text. The solid circles are extracted from measurements between 155° and 175° in the c.m. system. The curves calculated at 180° are taken from Ref. 8.

[1]A. K. Kerman and L. S. Kisslinger, Phys. Rev. 180, 1483 (1969).
[2]B. E. Bonner *et al.*, Phys. Rev. Lett. 39, 1253 (1977).
[3]N. S. Craigie and C. Wilkin, Nucl. Phys. B14, 477 (1969).
[4]T. Yao, Phys. Rev. 134, B454 (1964).
[5]G. W. Barry, Ann. Phys. (N.Y.) 73, 482 (1972).
[6]A. N. Anderson *et al.*, Phys. Rev. Lett. 40, 1553 (1978).
[7]E. Biegert *et al.*, Phys. Rev. Lett. 41, 1098 (1978).
[8]S. S. Vasan, Phys. Rev. D 8, 4092 (1973).
[9]G. D. Ohlsen, Rep. Prog. Phys. 35, 717 (1972).
[10]R. D. Klem *et al.*, Phys. Rev. Lett. 38, 1272 (1977).
[11]F. Seiler and E. Baumgartner, in *Proceedings of the Third International Symposium on Polarization Phenomena in Nuclear Reactions*, edited by H. H. Barschall and W. Haeberli (Madison, University of Wisconsin, 1970), p. 518.
[12]E. Parker, private communication.

Search for an Anomalously Heavy Isotope of Oxygen

R. Middleton, R. W. Zurmühle, J. Klein, and R. V. Kollarits
Department of Physics, University of Pennsylvania, Philadelphia, Pennsylvania 19104
(Received 21 May 1979)

A search has been made for an anomalously heavy isotope of oxygen spanning the mass range 20 to 54 amu with use of a tandem accelerator as an ultrasensitive mass spectrometer. An upper limit of heavy hadron to nucleon ratios was established at 10^{-16} over the entire mass region and over a large portion of it at 10^{-18}. This ratio is considerably lower than the predictions of cosmological models, namely $\sim 10^{-10}$ to 10^{-11}.

In a recent Letter, Dover, Gaisser, and Steigman[1] suggest the possibility that new stable heavy hadrons, proposed by several different elementary-particle theories,[2] should be present in $Z>1$ nuclei at levels of at least $\sim 10^{-10}$. In several specific models, these authors[1] further note that the stable hadron is electrically neutral and isoscalar and its mass is likely to be $\gtrsim 10$ GeV and most probably would be nonintegral (in amu). Since the particle is not anticipated to bind with a single proton to form a heavy isotope of hydrogen, the high sensitivity ($\sim 10^{-18}$ to 10^{-19}) searches of Muller, Alvarez, Holley, and Stephenson[3] and Alvager and Naumann[4] would, assuming its existence, have failed to detect it. The limits on anomalous nuclei of arbitrary mass in elements with $Z>1$ are much poorer, typically 10^{-6}.[5]

In view of the foregoing it was decided to use our FN tandem accelerator as an ultrasensitive mass spectrometer and to search for an anomalously heavy isotope of some element with $Z>1$. Although several elements were considered oxygen was chosen because (1) it readily forms a negative ion, (2) the dimer and trimer negative-ion beams are very weak, and (3) by using ^{18}O that had been enriched by gaseous diffusion one might expect to gain a factor of about at least 500 in sensitivity.

Experimental procedure.—Figure 1 shows schematically the modifications that have been made over the past year to our tandem accelerator for such studies. These include the addition of a second sputter source followed by a 90° analyzing magnet, a crossed-field velocity selector, and a removable detector located immediately prior to the image slits of the tandem's 90° analyzing magnet. The source magnet is double focusing with a radius of 30 cm and has a mass resolution $\Delta M/M$ of about 1/50 when the entrance and exit slits are adjusted to accept 90% of the available negative-ion current. The velocity selector is 50 cm long and is located immediately after the high-energy quadrupole magnet about 200 cm before the object slits. The $^{18}O^-$ beam was generated in the sputter source by spraying ^{18}O gas onto the surface of a high-purity titanium cone. The negative-ion current throughout the experiment was about 32 μA.

Preliminary measurements revealed that the most severe experimental difficulty was the extremely high count rate near the integer masses of 27 and above (frequently $>10^6$ counts/sec). Since calculations based on the tables of North-

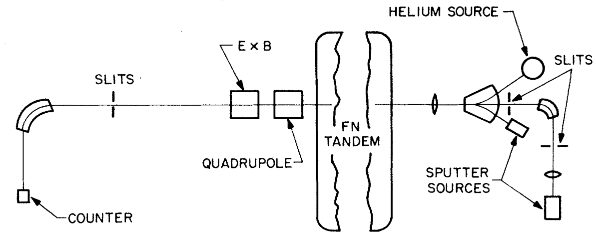

FIG. 1. General plan of FN tandem accelerator as used for supersensitive mass spectroscopy.

